



Publication Year	2015
Acceptance in OA @INAF	2020-06-08T11:20:23Z
Title	High Energy Spectral Evolution of V404 Cygni during the 2015 June Outburst as Observed by INTEGRAL
Authors	NATALUCCI, LORENZO; FIOCCHI, MARIATERESA; BAZZANO, ANGELA; UBERTINI, PIETRO; Roques, Jean-Pierre; et al.
DOI	10.1088/2041-8205/813/1/L21
Handle	http://hdl.handle.net/20.500.12386/25955
Journal	THE ASTROPHYSICAL JOURNAL LETTERS
Number	813

HIGH ENERGY SPECTRAL EVOLUTION OF V404 CYGNI DURING THE 2015 JUNE OUTBURST AS OBSERVED BY *INTEGRAL**

LORENZO NATALUCCI¹, MARIATERESA FIOCCHI¹, ANGELA BAZZANO¹, PIETRO UBERTINI¹,
JEAN-PIERRE ROQUES², AND ELISABETH JOURDAIN²

¹ Istituto di Astrofisica e Planetologia Spaziali, INAF, Via Fosso del Cavaliere 100, I-00133 Roma, Italy

² Université de Toulouse, UPS-OMP CNRS, IRAP, 9 Av. Colonel Roche, BP 44346, F-31028 Toulouse cedex 4, France
Received 2015 August 18; accepted 2015 October 8; published 2015 October 30

ABSTRACT

The black hole binary GS 2023+338 exhibited an unprecedentedly bright outburst in 2015 June. On 2015 June 17, the high energy instruments on board *INTEGRAL* detected an extremely variable emission during both bright and low luminosity phases, with dramatic variations of the hardness ratio on timescales of approximately seconds. The analysis of the IBIS and SPI data reveals the presence of hard spectra in the brightest phases, compatible with thermal Comptonization with a temperature of $kT_e \sim 40$ keV. The seed photon's temperature is best fit by $kT_0 \sim 7$ keV, which is too high to be compatible with blackbody emission from the disk. This result is consistent with the seed photons being provided by a different source, which we hypothesize to be a synchrotron driven component in the jet. During the brightest phase of flares, the hardness shows a complex pattern of correlation with flux, with the maximum energy released in the range of 40–100 keV. The hard-X-ray variability for $E > 50$ keV is correlated with flux variations in the softer band, showing that the overall source variability cannot originate entirely from absorption, but at least part of it is due to the central accreting source.

Key words: black hole physics – gamma rays: stars – radiation mechanisms: non-thermal – stars: individual (V404 Cygni, GS 2023+338) – X-rays: binaries

1. INTRODUCTION

The recurrent black hole binary GS 2023+338 (=V404 Cygni) went into outburst on 2015 June 15 after 26 years of quietness. A sudden increase in accretion rate was initially detected with the *Swift* satellite (Barthelmy et al. 2015) and reported also by *MAXI* (Negoro et al. 2015). Soon after these notifications, many ground and space facilities began following the event. Thanks to its exceptionally bright flux, V404 Cygni represents an excellent test laboratory at high energies, where it is possible to unveil the properties of the central engine thanks to the reduced absorption effect. V404 Cygni was detected for the first time in X-ray with the *Ginga* satellite in 1989 May 19 (Kitamoto et al. 1989; Makino 1989; Makino et al. 1989) and then observed with instruments on board the *Roentgen* observatory on Mir-Kvant for more than two months (Sunyaev et al. 1991). The authors reported on the emission spectra in the 2–300 KeV band at different epochs and different flux levels, with evidence of variability of the soft part ($E < 15$ keV). The source behavior was also followed up in optical and the system identified with V404 Cygni (Wagner et al. 1989), while the use of archival optical data allowed for the discovery of two outbursts in 1938 and 1956. The extensive monitoring of the source allowed for the determination of the key parameters of the system, having a mass function of 6.08 ± 0.06 (Casares & Charles 1994). The compact object is a $\sim 10 M_\odot$ black hole with an orbital period of 6.5 days and a $1 M_\odot$ K0IV companion (Casares et al. 1993). The best distance estimate is 2.39 ± 0.14 kpc (Miller-Jones et al. 2008). This source has been the best studied quiescent system, being also the most luminous stellar black hole in this state (Bradley et al. 2007; Hynes et al. 2009;

Rana et al. 2015). A spectral energy distribution with simultaneous coverage at X, UV, optical, and radio has been compiled, revealing an IR excess, which originated from either a cold disk or a jet (Hynes et al. 2009). The X-ray data from two epochs indicated a power-law continuum with an index of ~ 2 , with no indication of spectral variability in spite of a factor of 10 variation in luminosity. The radio data is consistent with a flat spectrum, resembling a typical X-ray binary's hard state and being associated with a compact jet; the radio variability is not correlated with X-ray variability.

On 2015 June 17, a public *INTEGRAL* Target of Opportunity (ToO) program started, and we report on the preliminary analysis of the collected data in this Letter.

2. OBSERVATIONS AND DATA ANALYSIS

V404 Cyg has been monitored at high energies by *INTEGRAL* (Winkler et al. 2003) and other space facilities by dedicated ToO programs (Ferrigno et al. 2015b; Gandhi et al. 2015; Kuulkers et al. 2015; Motta et al. 2015a, 2015b; Natalucci et al. 2015; Rodriguez et al. 2015b; Roques et al. 2015b; Segreto et al. 2015). An initial, extended phase with intense flaring and large, short-term variations in hardness (down to a few second timescales) occurred, with the source reaching luminosities of up to $\sim 5 \times 10^{38}$ erg s⁻¹. Most instruments sensitive in the X-ray band were saturated by such a high flux, see, e.g., King & Miller (2015). The peak intensity during five days of activity reached 44 Crab on MJD 57194.31 as detected by *INTEGRAL* (Rodriguez et al. 2015a). *INTEGRAL* has monitored the source quite continuously since 2015 June 17, with short (approximately half a day) interruptions due to operational constraints (mostly, scheduled for each perigee passage). Around 2015 June 28, the source had faded considerably (Ferrigno et al. 2015a) but remained visible at a level of a few mCrab intensity in the hard X-rays (Walton et al. 2015).

* *INTEGRAL* is an ESA project with instruments and science data centre funded by ESA member states (especially the PI countries: Denmark, France, Germany, Italy, Switzerland, Spain), Czech Republic and Poland, and with the participation of Russia and the USA.

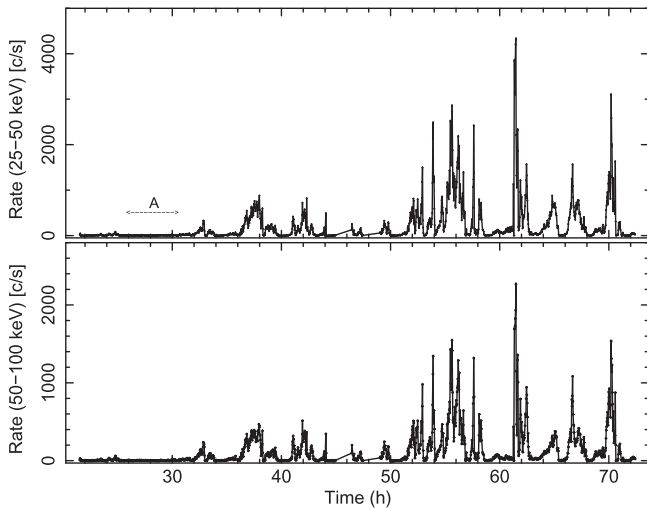


Figure 1. Light curve with IBIS/ISGRI count rates in the 25–50 keV and 50–100 keV energy bands, for the data period spanning revolution 1554. The start time is MJD 57190, UTC 21:30:45:186.

In this Letter, we analyze the spectral evolution of V404 Cygni during the intense initial flaring. We use *INTEGRAL* observations performed during revolution 1554, starting at MJD 57190.896 with a total elapsed time of 50.55 hr. This period is coincident with the starting phase of the *INTEGRAL* monitoring. The IBIS/ISGRI data for this observation are near real-time data processed using the latest release of the *INTEGRAL* Offline Scientific Analysis (OSA V10.1). This software has been used to obtain light curves and spectra in different common time intervals. SPI data are taken from the consolidated data archive, whereas their analysis makes use of specific tools developed at IRAP (Roques et al. 2015a).

The time evolution of the hard-X-ray emission from the source is shown in Figure 1. The hardness ratio (hereafter, HR) during the most turbulent phases varies on timescales down to at least a few seconds. In Figure 2, the intensity and hardness profiles are shown for the science window (hereafter, SCW) no. 43, where the source flux reached its maximum within our observing period. For the purpose of spectral analysis, we divided the time profile of the major flare into time intervals 100 s long, as shown in Figure 2, and built a total of six spectra by grouping the ones with similar HR and fluxes. In particular, we group spectra if their flux difference is $<20\%$ and the difference in HR is <0.05 . Together with the low-state spectrum of period A, this results in a set of seven spectra, A to G. For IBIS/ISGRI, the range 13–1000 keV was sampled using 85 channels with variable width, chosen according to a logarithmic law. We restricted the analysis to the range of 25–300 keV, for which there exists an accurate response.

3. RESULTS

The overall dependence of source hardness on hard-X-ray flux is shown in Figure 3. The distribution of values, when represented as the (normalized) difference of count rates in the 50–100 and 25–50 keV bands, reproduces the shape of a horse head. It is interesting to note that, while at low fluxes (below ~ 0.1 Crab) the hardness is varying on a wide scale, it is more stable at intermediate fluxes with a weak trend of being correlated with flux up to intensities below ~ 2 Crab. At higher fluxes, corresponding to the brightest flaring episodes, the

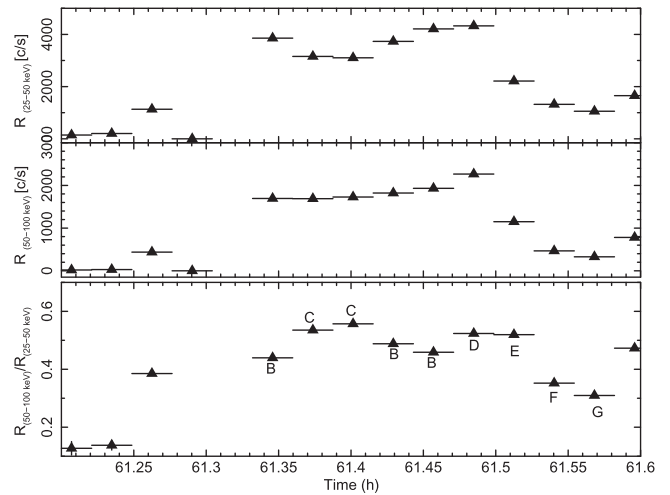


Figure 2. Light curves of the major flare in the 25–50 keV (top panel) and 50–100 keV (center panel) bands. Start time is MJD 57190, 21:30:45:186 UT. The hardness ratio in the two bands is shown in the bottom panel. Periods B to G mark the intervals used for the spectral analysis (see the text for details).

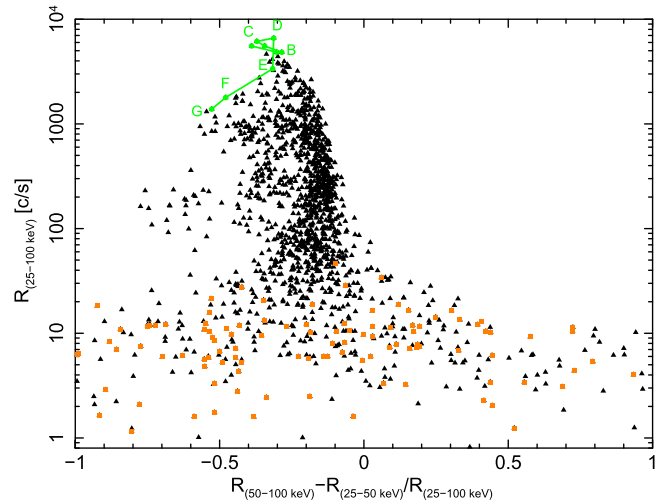


Figure 3. Intensity vs. hardness diagram for the full data set. Each point is generated using intensity values averaged over 100 s. Square orange points at the bottom are integrated on period A, whereas green circle points (B to G) are taken during the most intense flare.

hardness seems to be anticorrelated with flux. However, within a single X-ray flare, harder spectra may occur at higher fluxes, as it holds for the green points corresponding to the data for the brightest flare, which occurred within SCW 43 (intervals B to G). If this is the case, the anticorrelation HR-flux could hold for peak fluxes of different flare episodes and not during a single flare (see also Figure 4).

The IBIS/ISGRI data are affected by gaps due to limited telemetry bandwidth. The length of such gaps is of the order of a few seconds and their rate is slightly variable, being correlated with source intensity; due to this, the software actually reconstructs only a limited portion of spectral information for some of the 100 s long spectra. For this reason, we have been able to obtain a good match for IBIS and SPI data (i.e., same live time intervals) only for the periods A, F, and G.

The spectra shown in Figure 4 describe the evolution of the source emission during the low-state period (A) and the flare of

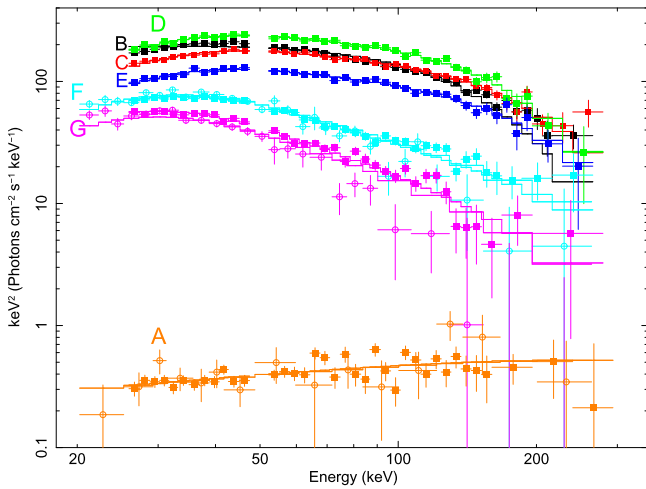


Figure 4. Spectra measured for different phases: a low-state spectrum (A) and spectra measured during the most intense flare (B to G). Circles denote data from SPI; squares from IBIS/ISGRI.

SCW 43 (B to G), as derived with IBIS/ISGRI and SPI. IBIS and SPI source fluxes have generally been found in good agreement ($\leq 12\%$), despite the strong source variability and the non-homogeneous data taking intervals for the two instruments. Furthermore, we found that, at high flux levels, the IBIS/ISGRI spectra appear systematically harder than SPI ones, yielding a difference in spectral index lower than $\sim 5\%$ – 10% . The reasons for this are under investigation; however, we have verified that the induced systematic effect on the spectral parameters is very small when fitting with physically motivated models.

The low-state spectrum measured for period A (see Figure 1) has been analyzed by performing a joint fit with both instruments. It can be modeled by a simple power law with photon index $\Gamma = 1.5 \pm 0.3$, with a lower limit for the high energy cutoff of ≈ 120 keV. The average flux is $1.8 \pm 0.1 \times 10^{-9}$ erg cm $^{-2}$ s $^{-1}$ in the 25–400 keV band, corresponding to a luminosity of $\sim 1.2 \times 10^{36}$ erg s $^{-1}$. The two instruments’ cross-normalization is 1.0 ± 0.1 .

The spectra during the main flare (B to G) show a prominent high-energy cutoff. A thermal Comptonization model, *comptt* in XSPEC, provides a satisfactory description of the data (see Table 1). For the highest fluxes, B to E, the temperature of the accreting plasma is quite constant around ~ 40 keV. After some flux decline (spectrum F) the electron temperature increases up to >100 keV and the optical depth decreases ($\tau < 0.1$). In all cases, the temperature of the seed photons for the Comptonization is high, around ~ 7 keV. We have verified that a model spectrum with a seed photon temperature of between 0.1 and 2 keV, typical of the thermal blackbody emission from an accretion disk, cannot reproduce the data within the thermal Comptonization model. Forcing the seed temperature to such low values, the fit requires a second additive component, which cannot be accounted for by reflection: in this case, modeling the spectra with a single direct continuum with reflection yields excessively high values of the reflection normalization, as we verified using both the *pexriv/pexrav* (Magdziarz & Zdziarski 1995) and *xillver* (Garcia et al. 2013) models. Conversely, if we adopt the single component model reported in Table 1, the use of reflection does not improve the fit results, with the exception of spectrum C, for which fitting the data

Table 1
Results of Spectra Fitting Using the *Comptt* Model

Spec. Id ^a	kT_0 (keV)	kT_e (keV)	τ	Flux ^b	χ^2/dof
B	7.05 ± 0.2	42_{-4}^{+7}	$0.7_{-0.2}^{+0.1}$	5.5	25.8/38
C	7.4 ± 0.2	40_{-3}^{+5}	1.0 ± 0.16	5.0	54.9/39
C _R ^c	$8.6_{-1.4}^{+1.0}$	42_{-18}^{+8}	0.9 ± 0.3	5.0	40.3/36
D	7.2 ± 0.3	34_{-2}^{+3}	1.2 ± 0.2	6.6	42.0/37
E	7.4 ± 0.3	41_{-5}^{+11}	$0.9_{-0.3}^{+0.2}$	3.5	37.9/38
F ^(*)	6.4 ± 0.2	182_{-93}^{+8}	<0.09	1.73 ^d	91.5/73
G ^(*)	6.0 ± 0.3	63_{-33}^{+88}	<0.7	1.76 ^e	101.3/66
				1.17 ^d	
				1.04 ^e	

Notes.

^a Fits with IBIS and SPI spectra are marked by (*). In all other cases, only IBIS data have been used.

^b Flux values in units of 10^{-7} erg s $^{-1}$ cm $^{-2}$, in the 20–200 keV range.

^c Fit with added reflection component (see the text for more details).

^d Flux measured by IBIS.

^e Flux measured by SPI.

with an added *xillver* component yields a significantly better result ($\chi_{\text{red}}^2 = 1.12$ instead of 1.41). In this case, the fraction of reflected flux is found to be $\approx 22\%$.

Concerning our detection of the ~ 7 keV soft component, we considered effects that could modify the shape of the spectrum at the lowest energies, like partial covering of the central X-ray source. King et al. (2015) reported about two soft-X-ray observations with *Chandra* taken on June 22 and 23, when V404 Cygni was still active with average 2–10 keV fluxes of 9.5×10^{-9} erg cm $^{-2}$ s $^{-1}$ and 1.3×10^{-8} erg cm $^{-2}$ s $^{-1}$, respectively. The detection of strong narrow emission lines led the authors to conclude that the central source is obscured, with evidence for the line formation region to be located at distances greater than 7×10^9 cm, possibly coincident with the outer disk. Motivated by this result, we used a partial covering absorber (*pcfabs*) to model our flare spectra (B to G), in conjunction with the usual *comptt* component. As expected, we obtain very large errors in the parameters characterizing the low-energy spectrum, i.e., the covering fraction F_{cov} , the related absorption column, N_{H} , and the seed temperature kT_0 . Nevertheless, if we impose values of kT_0 lower than 2 keV in these fits, the N_{H} values are always far too high, i.e., typically between 5×10^{24} cm $^{-2}$ and 3×10^{25} cm $^{-2}$ for values of F_{cov} from 0.20 to unity. We conclude that the partial covering of the source does not affect our main result about the observed high temperature of the seed photon spectrum.

Finally, fitting the IBIS/ISGRI data with the hybrid thermal/non-thermal Comptonization model *eqpair* (Coppi 1999) also yields good results: $\chi^2/\text{dof} = 48.6/37$ and $25.9/37$ for spectrum C and spectrum F, respectively. Spectrum C requires high values of the reflection normalization ($\Omega/2\pi \sim 1$). The temperature of the seed photon distribution for the above fits is $kT_{\text{bb}} = 6.2_{-0.4}^{+0.9}$ and $kT_{\text{bb}} = 7.6_{-0.9}^{+0.5}$, respectively, essentially in good agreement with the *comptt* model.

4. DISCUSSION

V404 Cygni is an established transient black hole binary, for which two bright outbursts have been available for study in the hard X-rays. On the basis of its behavior in the previous 1989 outburst, it had been proposed (Tomsick 2004) that it belongs

to a class of transient sources for which the spectral state is quite independent on luminosity. Figure 3 confirms this picture as a general trend also for this most recent event, at least for source luminosities above $\sim 10^{36}$ erg s $^{-1}$.

One of the questions concerns the origin of the X-ray variability, i.e., is this related to rapid changes in the accretion flow, to a variable component from a jet, or both? From the hard-X-ray data we can exclude that the variability is totally due to absorption by a disk outflow or wind. Whereas in the soft X-rays the central source could be partially or totally obscured (King et al. 2015), using the hard X-rays we are unveiling the variability component of the central accreting region, as proven by the rapid and large intensity fluctuations detected at energies up to >100 keV.

During the current outburst of V404 Cygni, we observed that the spectrum of the main flare is actually described by Comptonization of a thermal plasma. The size of the corona can be estimated following the approach of Merloni & Fabian (2001) using our measured parameters of temperature, accretion rate, luminosity, and optical depth. If the energy of the corona is purely thermal, its size would be of the order of $\sim 10^4$ Schwarzschild radii (R_s). Conversely, if the stored energy is mainly present as a magnetic field, the size would be of the order of a few R_s . Such a compact corona could explain, in our case, the almost constant plasma temperature of ~ 40 keV, which is observed in all high flux spectra of the main flare. This scenario could also favor the possibility that the seed photons are not injected by the accretion disk, but have different origins as imposed by their high temperature of ~ 7 keV. The seed photons could be provided by a moderately optically thick synchrotron source within the jet, giving rise to a self-absorbed spectrum. This radiation would then be upscattered by the surrounding hot corona. For reference, a scenario with synchrotron generated seed photons has been discussed by Wardzinski & Zdziarski (2000).

Finally, we note that our spectral results are not affected by instrumental effects due to the exceptionally high count rate from V404 Cygni. In fact, they are in agreement with the spectral analysis reported by Roques et al. (2015a) using the SPI data for the same observations. The SPI and IBIS/ISGRI detectors are based on completely different technology and are cross-calibrated in-flight using the Crab Nebula as reference source.

5. CONCLUSIONS

We have analyzed *INTEGRAL* data from the initial phase (first pointing with *INTEGRAL*) of the V404 Cygni recent outburst. The source features high flux variability and hard spectra even in the brightest flares, with evidence for a thermally Comptonized spectrum with a plasma temperature of ~ 40 keV. The spectral parameters of the analysis must be taken with caution due to the intrinsic limitations of the models; there is an indication of a seed photon component not coincident with the hot accretion disk thermal photons.

Through this study, we characterize the high energy behavior of the source at the highest fluxes, where the hardness during single flares is correlated with flux (see Figure 4) up to luminosities of a few percent of Eddington and anti-correlated at higher fluxes. The general behavior in hard X-rays is in agreement with the spectral variability of the source detected in the previous 1989 outburst (Sunyaev et al. 1991).

The Italian authors acknowledge ASI/INAF agreement No. 2013-025-R.0 and thank M. Federici for the setup and maintenance of the *INTEGRAL* archive and analysis S/W at IAPS. The *INTEGRAL*/SPI project has been completed under the responsibility and leadership of CNES. We are grateful to ASI, CEA, CNES, DLR, ESA, INTA, NASA, and OSTC for support. We also thank the anonymous referee for precious suggestions.

REFERENCES

- Barthelmy, S. D., D’Ai, A., D’Avanzo, P., et al. 2015, GCN, 17929, 1
Bradley, C. K., Hynes, R. I., Kong, A. K. H., et al. 2007, *ApJ*, 667, 427
Casares, J., & Charles, P. A. 1994, *MNRAS*, 271, L5
Casares, J., Charles, P. A., Naylor, T., & Pavlenko, E. P. 1993, *MNRAS*, 265, 834
Coppi, P. S. 1999, in ASP Conf. Ser. 161, High Energy Processes in Accreting Black Holes, ed. J. Poutanen & R. Svensson (San Francisco, CA: ASP), 375
Ferrigno, C., Bozzo, E., Boissay, R., et al. 2015a, ATel, 7731
Ferrigno, C., Fotopoulou, S., Domingo, A., et al. 2015b, ATel, 7662
Gandhi, P., Shaw, A. W., Pahari, M., et al. 2015, ATel, 7727
Garcia, J., Dauser, T., Reynolds, C. S., et al. 2013, *ApJ*, 768, 146
Hynes, R. I., Bradley, C. K., Rupen, M., et al. 2009, *MNRAS*, 399, 2239
King, A. L., & Miller, J. M. 2015, ATel, 7745
King, A. L., Miller, J. M., Raymond, J., Reynolds, M. T., & Morningstar, W. 2015, *ApJL*, submitted (arXiv:1508.01181)
Kitamoto, S., Tsunemi, H., Miyamoto, S., et al. 1989, *Natur*, 342, 518
Kuulkers, E., Motta, S., Kajava, J., et al. 2015, ATel, 7647
Magdziarz, P., & Zdziarski, A. A. 1995, *MNRAS*, 273, 837
Makino, F. 1989, IAUC, 4782, 1
Makino, F., Wagner, R. M., Starrfield, S., et al. 1989, IAUC, 4786, 1
Merloni, A., & Fabian, A. C. 2001, *MNRAS*, 321, 549
Miller-Jones, J. C. A., Gallo, E., Rupen, M. P., et al. 2008, *MNRAS*, 388, 1751
Motta, S., Beardmore, A., Kuulkers, E., & Altamirano, D. 2015a, ATel, 7694
Motta, S., Beardmore, A., Oates, S., et al. 2015b, ATel, 7665
Natalucci, L., Focchi, M., Bazzano, A., Ubertini, P., & Kuulkers, E. 2015, ATel, 7759
Negoro, H., Matsumitsu, T., Mihara, T., et al. 2015, ATel, 7646
Rana, V., Loh, A., Corbel, S., et al. 2015, *ApJ*, submitted (arXiv:1507.04049)
Rodriguez, J., Cadolle Bel, M., Alfonso-Garzon, J., et al. 2015a, *A&A*, 581, L9
Rodriguez, J., Ferrigno, C., Cadolle Bel, M., et al. 2015b, ATel, 7702
Roques, J. P., Jourdain, E., Bazzano, A., et al. 2015a, *ApJL*, in press (arXiv:1510.03677)
Roques, J. P., Jourdain, E., & Kuulkers, E. 2015b, ATel, 7693
Segreto, A., Del Santo, M., D’Ai, A., et al. 2015, ATel, 7755
Sunyaev, R., Kaniiovskii, A. S., Efremov, V. A., et al. 1991, *SvAL*, 17, 123
Tomsick, J. A. 2004, Proc. “X-Ray Timing 2003: Rossi and Beyond”, ed. P. Kaaret, F. K. Lamb, & J. H. Swank (Melville, NY: AIP), 71
Wagner, M., Starrfield, S., & Cassatella, A. 1989, IAUC, 4783
Walton, D., Harrison, F., Forster, K., et al. 2015, ATel, 7797
Wardzinski, G., & Zdziarski, A. 2000, *MNRAS*, 314, 183
Winkler, C., Courvoisier, T. J. L., Di Cocco, G., et al. 2003, *A&A*, 411, L1